TASK QUARTERLY 10 No 2, 207–220

IMPLEMENTATION OF CONTINUUM DAMAGE IN ELASTO-VISCOPLASTIC CONSTITUTIVE EQUATIONS

ANDRZEJ AMBROZIAK[1], PAWEŁ KŁOSOWSKI[1], MICHAŁ NOWICKI[1] AND RÜDIGER SCHMIDT[2]

[1] *Faculty of Civil and Environmental Engineering, Gdansk University of Technology, Narutowicza 11/12, 80-952 Gdansk, Poland* {*ambrozan, klosow, mnowicki*}*@pg.gda.pl*

[2] *Department of General Mechanics, RWTH Aachen University, Templergraben 64, 52056 Aachen, Germany schmidt@iam.rwth-aachen.de*

(Received 02 January 2006; revised manuscript received 26 March 2006)

Abstract: Modelling of the continuum damage framework is developed for application in the elasto-viscoplastic Chaboche constitutive model. A brief description of the basic variant of the Chaboche model equations is given, followed by a discussion of the most important assumptions necessary to obtain evolution of the continuum damage model and its application to the open FE commercial program. A consistent presentation of the two proposed approaches is followed by numerical examples.

Keywords: elasto-viscoplastic constitutive models, damage, finite element method

1. Introduction

The first order differential equations describing the evolution of viscous effects and hardening was proposed in the 1960's by Perzyna [1]. It is one of the oldest modern elasto-viscoplastic models, still often used in material descriptions of many engineering applications due to its simplicity related to a small number of material parameters and a straightforward identification procedure. The Chaboche model is an extension of Perzyna's law [2]. In the basic variant of the Chaboche model seven inelastic material parameters have to be specified (see *e.g.* [3]). These model equations have been modified and developed many times (see *e.g.* [4], where several variants and their practical engineering applications are presented).

The main goal of the present paper is to present an application of the elasto-viscoplastic Chaboche model with isotropic damage evolution to the geometrically non-linear finite element analysis of plate and shell structures in the MSC.Marc

commercial code. The authors have taken advantage of the possibility of user-defined subroutines application in this code and introduced two ways of damage implementation in the Chaboche model.

2. Introduction to continuum damage modelling

The constitutive equations used in the present study are based on additive decomposition of strain rates for an isotropic material into the elastic, $\dot{\boldsymbol{\varepsilon}}^E$, and inelastic part, $\dot{\boldsymbol{\varepsilon}}^I$, in the form of

$$\dot{\boldsymbol{\varepsilon}} = \dot{\boldsymbol{\varepsilon}}^E + \dot{\boldsymbol{\varepsilon}}^I, \tag{1}$$

where the dots denote differentiation with respect to time.

The relation between stress and strain rates is defined by the following equation [5]:

$$\dot{\boldsymbol{S}} = (1-D)\,\boldsymbol{D} : \dot{\boldsymbol{\varepsilon}}^E = \tilde{\boldsymbol{D}} : \left(\dot{\boldsymbol{\varepsilon}} - \dot{\boldsymbol{\varepsilon}}^I\right), \tag{2}$$

where $\boldsymbol{D}$ is the elasticity tensor of the undamaged material, and $D \in \langle 0, 1)$ is the damage scalar parameter. Isotropic damage evolution is assumed, with cracks and cavities appearing during deformation distributed uniformly throughout the body's volume.

The concept proposed by Lemaitre [5] is used in the present paper to describe isotropic damage evolution. It should be noted that the Lemaitre proposal of damage evolution is not the only to be found in the literature (see *e.g.* Bonora [6], Chandrakanth [7] and [8], Dhar [9], Tai [10], Wang [11], Xiao [12], *etc.*). Lemaitre [5] has assumed that damage evolution can be expressed by the equation:

$$\dot{D} = \left(\frac{-Y}{S}\right)^s \dot{p}, \tag{3}$$

where S and s are the damage material parameters, while $\dot{p}$ is the rate of equivalent plastic strain, defined as:

$$\dot{p} = \sqrt{\dot{\boldsymbol{\varepsilon}}^I : \dot{\boldsymbol{\varepsilon}}^I}. \tag{4}$$

The Y function, called the damage strain energy release rate, is given by:

$$-Y = \frac{1}{2(1-D)^2 E}\left(\frac{2}{3}(1+\nu)\sigma_{eq}^2 + 3(1-2\nu)\sigma_H^2\right), \tag{5}$$

where E and ν are Young's modulus and Poisson's ratio of the undamaged material, σ_{eq} and σ_H is the Huber-Mises equivalent and hydrostatic stress.

3. Chaboche model description

In the Chaboche model (see *e.g.* [2, 13]) the inelastic strain rate has the following form:

$$\dot{\boldsymbol{\varepsilon}}^I = \frac{3}{2}\dot{p}\frac{\boldsymbol{S}' - \boldsymbol{X}'}{J(\boldsymbol{S}' - \boldsymbol{X}')}, \tag{6}$$

where $J(\boldsymbol{a}) = \sqrt{\frac{3}{2}\boldsymbol{a} : \boldsymbol{a}} = \sqrt{\frac{3}{2}a^{ij}a_{ij}}$, while $\boldsymbol{S}'$ and $\boldsymbol{X}'$ are the deviatoric parts of the stress and back stress tensors, respectively.

The isotropic damage expressed by the scalar parameter is considered to be $0 \leq D < 1$. The $\dot{p}$ rate in the Chaboche model with damage is defined as follows [14]:

$$\dot{p} = \left\langle \frac{(J(\boldsymbol{S}' - \boldsymbol{X}')/(1-D)) - R - k}{K} \right\rangle^n, \tag{7}$$

where k, D and K, n are the initial yield stress, the damage parameter and the viscous material parameters. The angle brackets, $\langle x \rangle$, are referred to as the McCauley brackets and are defined as $\langle x \rangle = \frac{1}{2}(x + |x|)$. The kinematic hardening tensor, $\boldsymbol{X}$, and the isotropic hardening scalar function, R, are defined in the differential form:

$$\dot{R} = b(R_1 - R)\dot{p} \quad , \quad \dot{\boldsymbol{X}} = \frac{2}{3} a \dot{\boldsymbol{\varepsilon}}^I - c \boldsymbol{X} \dot{p}, \tag{8}$$

where b, R_1, a and c are hardening evolution material parameters.

The material parameters' identification process for the Chaboche model with damage has been described by Ammar and Dufailly [14]. They have specified the elastic and inelastic material parameters for viscoplastic law and established the damage material parameters in an iterative way.

4. Description of the applied program and subroutines used

4.1. MSC.Marc

The MSC.Marc system has been used for the present numerical calculations. It is a multipurpose finite element system of programs for advanced engineering simulations. Its great advantage is the possibility to apply over 100 modifiable user subroutines. The UVSCPL (viscoplastic modelling), USHELL (change of the element's thickness) and UACTIV (deactivation of finite elements) user subroutines [15] have been applied in the present study.

The standard MSC.Marc system supports the Chaboche model, but not in its variant with damage. The UVSCPL user-defined subroutine [15] has been used to introduce the Chaboche model with continuous damage into the MSC.Marc system. It should be noted that this routine enables very general description of viscoplastic material laws, which can be included in both static and dynamic calculations. This subroutine (without the USHELL and UACTIV routines) has also been successfully applied by Ambroziak in paper [16] to implement the Chaboche model with damage.

4.2. Numerical concepts of the damage approach

Two calculation variants are studied in the present investigations. In one of them, damage evolution is calculated according to the classic Chaboche-Lamaitre equations given in Section 2. In the other, damage evolution is not directly used in the Chaboche equations, but the change of the damage parameter generates change in the element's thickness. In this approach, the USHELL subroutine [15] is used to change the thickness of an element. This user subroutine allows specification of the shell elements' thickness for each integration point at any moment of the calculations. The main parts of the algorithms used in the computations are presented in Figures 1 and 2.

UVSCPL

$$\Delta \boldsymbol{X} = \frac{\Delta t}{2} \cdot \left(\dot{\boldsymbol{X}}_{t-\Delta t} + \dot{\boldsymbol{X}}_t \right), \quad \boldsymbol{X}_t = \boldsymbol{X}_{t-\Delta t} + \Delta \boldsymbol{X}$$

$$\Delta R = \frac{\Delta t}{2} \cdot \left(\dot{R}_{t-\Delta t} + \dot{R}_t \right), \quad R_t = R_{t-\Delta t} + \Delta R$$

$$\Delta D = \frac{\Delta t}{2} \cdot \left(\dot{D}_{t-\Delta t} + \dot{D}_t \right), \quad D_t = D_{t-\Delta t} + \Delta D$$

$$\boldsymbol{S}'_t,\ \boldsymbol{X}'_t,\ J\left(\boldsymbol{S}'_t - \boldsymbol{X}'_t\right),\ J\left(\boldsymbol{S}'_t\right),\ \mathrm{tr}\left(\boldsymbol{S}_t\right),\ \sigma_{eq},\ \sigma_H$$

$$\dot{p}_t = \left\langle \frac{\frac{J\left(\boldsymbol{S}'_t - \boldsymbol{X}'_t\right)}{1-D_t} - R_t - k}{K} \right\rangle^n$$

$$\dot{\boldsymbol{\varepsilon}}^I_t = \frac{3}{2} \cdot \dot{p}_t \cdot \frac{\left(\boldsymbol{S}'_t - \boldsymbol{X}'_t\right)}{J\left(\boldsymbol{S}'_t - \boldsymbol{X}'_t\right)}$$

$$\dot{\boldsymbol{X}}_t = \frac{3}{2} \cdot a \cdot \dot{\boldsymbol{\varepsilon}}^I_t - c \cdot \boldsymbol{X}_t \cdot \dot{p}_t$$

$$\dot{R}_t = b \cdot \left(R_1 - R_t\right) \cdot \dot{p}_t$$

$$Y_t = \frac{\sigma^2_{eq}}{2 \cdot \left(1 - D_t\right)^2 \cdot E} \cdot \left(\frac{2}{3} \cdot (1+v) + 3 \cdot (1-2 \cdot v) \cdot \left(\frac{\sigma_H}{\sigma_{eq}} \right)^2 \right)$$

$$\dot{D}_t = \left(\frac{Y_t}{S} \right)^S \cdot \dot{p}_t$$

$$\tilde{\boldsymbol{D}}_t = \left(1 - D_t\right) \cdot \boldsymbol{D}$$

$$\Delta \boldsymbol{\varepsilon}^I_t = \dot{\boldsymbol{\varepsilon}}^I_t \cdot \Delta t$$

$$\Delta \boldsymbol{S}_t = \tilde{\boldsymbol{D}}_t \cdot \left(\Delta \boldsymbol{\varepsilon}_t - \Delta \boldsymbol{\varepsilon}^I_t \right)$$
$$\boldsymbol{S}_{t+\Delta t} = \boldsymbol{S}_t + \Delta \boldsymbol{S}_t$$

UACTIV

if $(D_t \geq D_{cr})$ deactivate element

Figure 1. Flow graph of the main operations of the classical Chaboche-Lamaiter approach with UVSCPL + UACTIV subroutines

In the traditional numerical calculations of the shell and plate structures, the damage is also introduced by reduction of Young's modulus of the undamaged material:

$$\tilde{E} = E \cdot (1 - D). \tag{9}$$

UVSCPL

$$\Delta \boldsymbol{X} = \frac{\Delta t}{2} \cdot \left(\dot{\boldsymbol{X}}_{t-\Delta t} + \dot{\boldsymbol{X}}_t \right), \quad \boldsymbol{X}_t = \boldsymbol{X}_{t-\Delta t} + \Delta \boldsymbol{X}$$
$$\Delta R = \frac{\Delta t}{2} \cdot \left(\dot{R}_{t-\Delta t} + \dot{R}_t \right), \quad R_t = R_{t-\Delta t} + \Delta R$$

$$\boldsymbol{S}'_t,\ \boldsymbol{X}'_t,\ J\left(\boldsymbol{S}'_t - \boldsymbol{X}'_t\right),\ J\left(\boldsymbol{S}'_t\right),\ \mathrm{tr}\left(\boldsymbol{S}_t\right)$$

$$\dot{p}_t = \left\langle \frac{J\left(\boldsymbol{S}'_t - \boldsymbol{X}'_t\right) - R_t - k}{K} \right\rangle^n$$

$$\dot{\boldsymbol{\varepsilon}}^I_t = \frac{3}{2} \cdot \dot{p}_t \cdot \frac{\left(\boldsymbol{S}'_t - \boldsymbol{X}'_t\right)}{J\left(\boldsymbol{S}'_t - \boldsymbol{X}'_t\right)}$$

$$\dot{\boldsymbol{X}}_t = \frac{3}{2} \cdot a \cdot \dot{\boldsymbol{\varepsilon}}^I_t - c \cdot \boldsymbol{X}_t \cdot \dot{p}_t$$

$$\dot{R}_t = b \cdot \left(R_1 - R_t\right) \cdot \dot{p}_t$$

$$\Delta \boldsymbol{\varepsilon}^I_t = \dot{\boldsymbol{\varepsilon}}^I_t \cdot \Delta t$$

$$\Delta \boldsymbol{S}_t = \boldsymbol{D}_t \cdot \left(\Delta \boldsymbol{\varepsilon}_t - \Delta \boldsymbol{\varepsilon}^I_t\right)$$
$$\boldsymbol{S}_{t+\Delta t} = \boldsymbol{S}_t + \Delta \boldsymbol{S}_t$$

USHELL

$$\Delta D = \frac{\Delta t}{2} \cdot \left(\dot{D}_{t-\Delta t} + \dot{D}_t \right)$$

$$Y_t = \frac{\sigma^2_{eq}}{2 \cdot \left(1 - D_t\right)^2 \cdot E} \cdot \left(\frac{2}{3} \cdot (1 + v) + 3 \cdot (1 - 2 \cdot v) \cdot \left(\frac{\sigma_H}{\sigma_{eq}} \right)^2 \right)$$

$$\dot{D}_t = \left(\frac{Y_t}{S} \right)^S \cdot \dot{p}_t$$

$$D_t = D_{t-\Delta t} + \Delta D$$

$$\tilde{h}_t = \left(1 - \bar{D}_t\right) \cdot h_0$$

UACTIV

if $(D_t \geq D_{cr})$ deactivate element

Figure 2. Flow graph of the approach with changing element thickness with UVSCPL + USHELL + UACTIV subroutines

The authors propose that damage can be introduced by reduction of the element's initial thickness:

$$h = \left(1 - \bar{D}\right) \cdot h_0, \tag{10}$$

where h_0 is the element's initial thickness (constant for the whole element).

This approach (reduction of the element's thickness, USHELL) can only be used in the MSC.Marc system with shell elements. It should be noted that the current value of damage parameter D_i is different at each integration point of the current element in each layer i. As it is impossible to reduce the thickness of each layer of a finite element in numerical calculations, the average value of damage parameter $\bar{D}$ has been calculated as:

$$\bar{D} = \frac{1}{n} \sum_{i=1}^{n} D_i. \tag{11}$$

Finally, the current thickness of the damaged element at integration point has been evaluated according to Equation (10).

Four-node isoparametric shell elements divided into several layers have been used in the calculations. A 2×2 mesh of Gauss integration points has been applied for integration. The Newmark integration in time scheme has been utilized in the dynamic calculations, and the analysis has been focused on the evolution of damage parameter D. A rapid increase of this parameter, even at a single integration point in a single layer, can cause a numerical collapse of the calculations, even though the structure itself is still able to carry larger load. To avoid this numerical disadvantage, the authors have limited the maximum value of this parameter to $D_{cr} = 0.9$.

The alternative method of extending the calculations' range is deactivation of finite elements with high degree of damage. It has been determined that if the value of damage parameter D at all integration points of the element is greater than 0.5, the element is deactivated by the UACTIV subroutine [15]. It is worth pointing out that a deactivated element does not contribute to the load, mass, stiffness, or internal force calculations. This subroutine in the MSC.Marc system is always called at the beginning and at the end of each increment. Deactivation of finite elements alters the plate mass, which is not a physical effect. The authors intend develop the model further in order to eliminate this disadvantage.

Additionally, the re-meshing feature of the MSC.Marc system was utilised in each case. From several re-meshing criteria, the equivalent plastic strain criteria were selected. The element in which the equivalent plastic strain reached the value of 0.05 was subdivided into 4 elements. Only a single level of division was assumed, which means that elements from the first division could not be divided any more. This approach creates additional nodes but, unlike the nodes of the original mesh, they are not independent. Their translations and rotations are calculated on the basis of nodes of the virgin mesh.

Vanishing of elements can lead to a situation, when no element is attached to a certain node. If this happens to a node from the virgin mesh, the calculations will be broken due to this node's rigid movement. The opposite is the case with re-meshing nodes. As they are linked to the nodes of the original mesh, their displacements can be calculated even with no element attached. To avoid the problem of the original

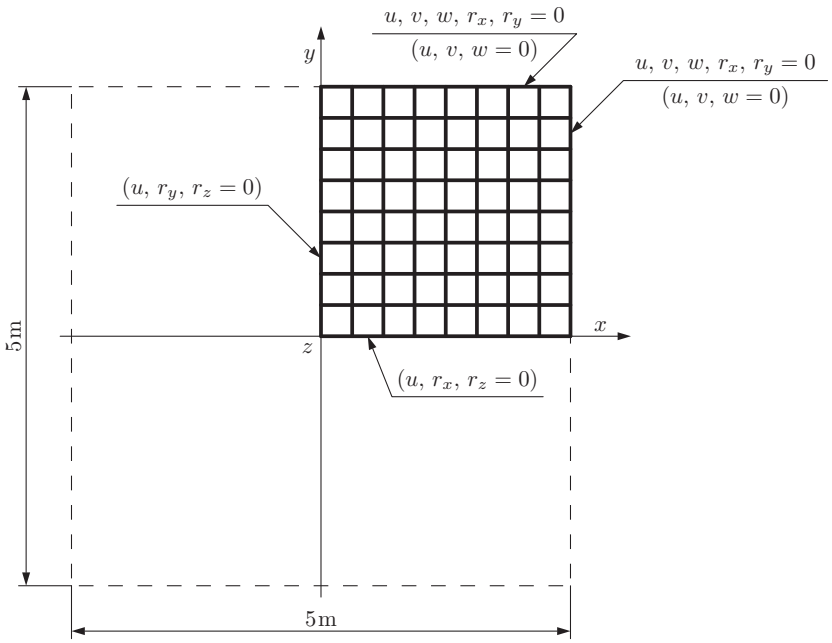

Figure 3. Geometry of a plate and its finite element mesh

mesh nodes' separation, weak spring supports can be added, which will have negligible influence on vibrations, but will protect a node against large rigid movement.

5. Numerical examples

Geometrically non-linear numerical calculations of the square plate presented in Figure 3 are performed. Due to the symmetry of the plate's geometry and loading, a quarter of the plate is discretized by a four-node thin-shell element (Element 139 [17]). Shell elements of total initial thickness $h_0 = 0.01\,\mathrm{m}$ are divided into five layers. The following material parameters are taken for the Chaboche model with damage (INCO alloy at 627°C from [14]): $E = 162.0\,\mathrm{GPa}$, $\nu = 0.3$, $k = 501.0\,\mathrm{MPa}$, $b = 15.0$, $R_1 = -165.4\,\mathrm{MPa}$, $a = 80.0\,\mathrm{GPa}$, $c = 200.0$, $n = 2.4$, $K = 12790.0\,(\mathrm{MPa{\cdot}s})^{1/n}$, $S = 4.48\,\mathrm{MPa}$, $s = 3.0$. The mass density is $\rho = 7900\,\mathrm{kg/m^3}$.

The loading (uniformly distributed pressure $p_{\max} = 1.5\,\mathrm{MPa}$) is increasing linearly from $p(t = 0.0\mathrm{s}) = 0$ to $p(t \geq 0.01\mathrm{s}) = p_{\max}$ and then remains constant. The non-linear equations of motion are integrated by the Newmark algorithm [18] with a time step of $\Delta t = 2.66 \cdot 10^{-4}\,\mathrm{s}$. Two variants of boundary conditions are investigated: hinged and clamped plate edges.

5.1. Case 1: a hinged plate

Screenshots of vertical displacement for the plate's quarter are presented in Figures 4 and 5. In the early stage of vibrations, re-meshing of the elements occurs, starting from the plate's edges – an effect of inertia of the middle part of the plate in dynamic calculations. Then, due to evolution of the damage parameters, elements close to the symmetry line elements are deactivated. Subsequently, the "crack" runs diagonally across the plate and, finally, the middle part of the plate

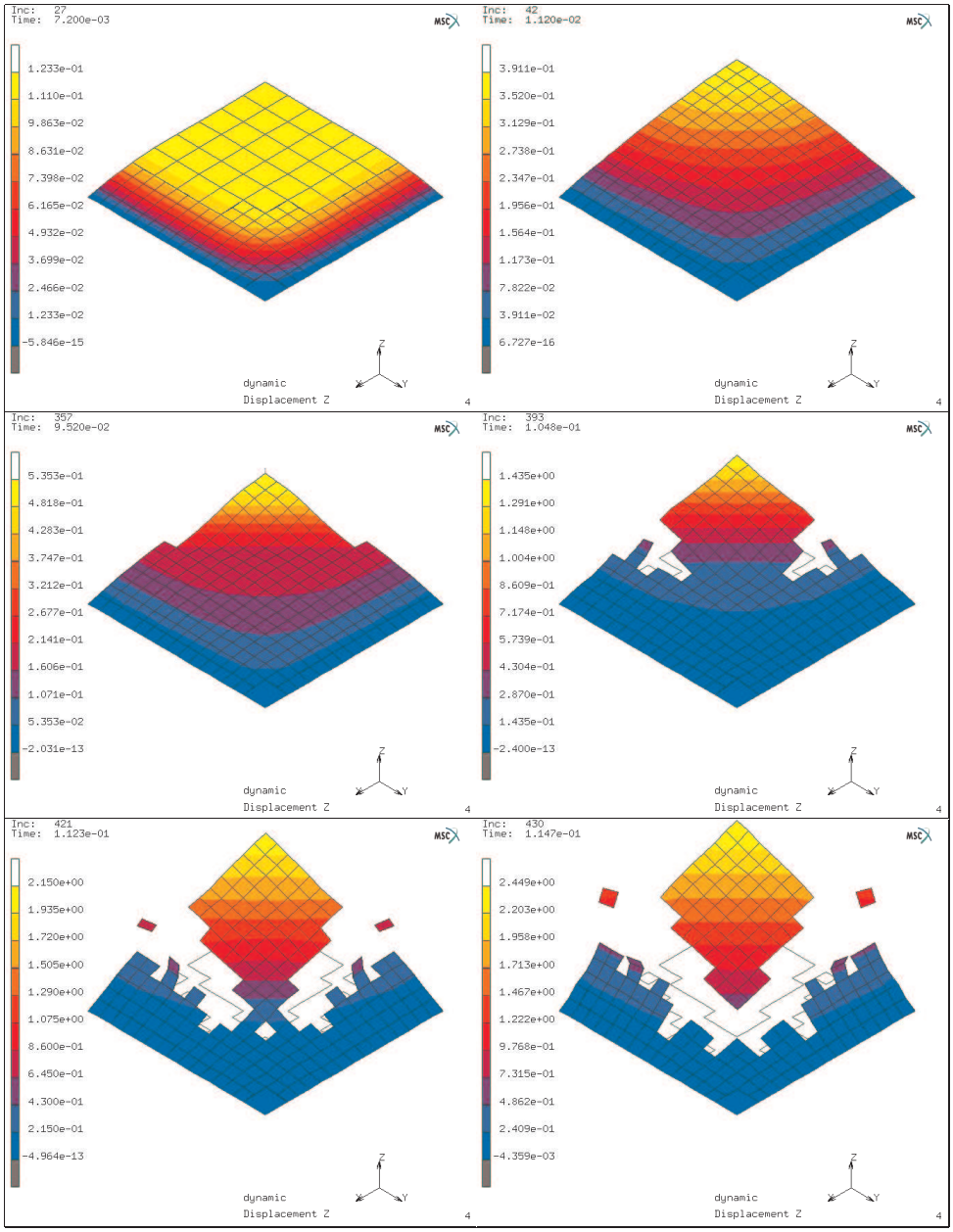

Figure 4. Hinged plate: damage analysis with subroutines UVSCPL + UACTIV ($t_1 = 7.2 \cdot 10^{-3}$ s, $t_2 = 1.12 \cdot 10^{-2}$ s, $t_3 = 9.52 \cdot 10^{-2}$ s, $t_4 = 1.048 \cdot 10^{-1}$ s, $t_5 = 1.123 \cdot 10^{-1}$ s, $t_6 = 1.147 \cdot 10^{-1}$ s)

is separated and moves rigidly. The history of the plate's damage is similar for both approaches, the only difference being that the separated part of the plate is smaller in the change of thickness concept. As the first deactivated element is the only one attached to the middle node of the plate, being a virgin mesh node, an additional weak spring has been attached to the plate in the Z axis' direction to eliminate rigid movement.

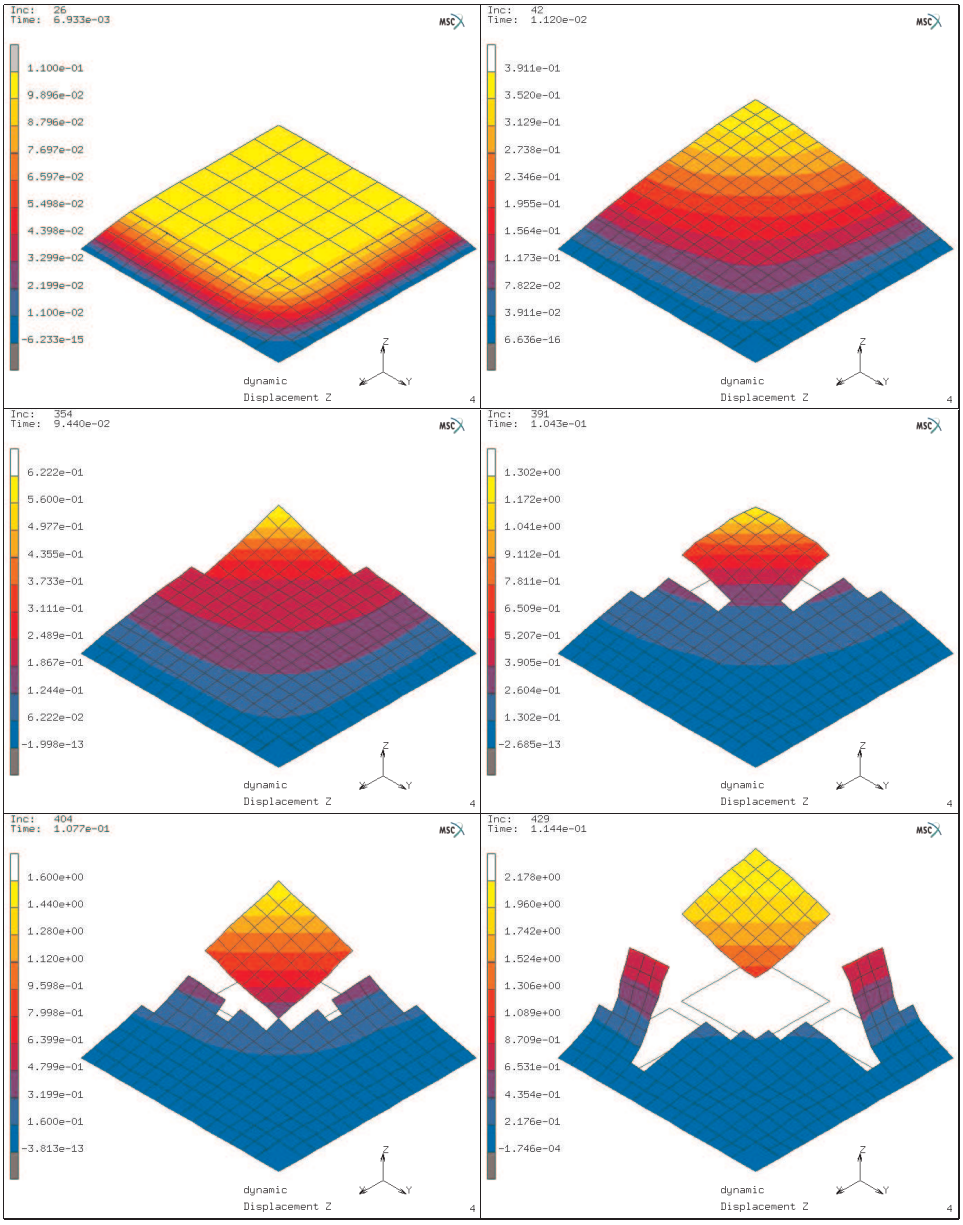

Figure 5. Hinged plate: damage analysis with subroutines UVSCPL + USHELL + UACTIV ($t_1 = 6.933 \cdot 10^{-3}$ s, $t_2 = 1.12 \cdot 10^{-2}$ s, $t_3 = 9.44 \cdot 10^{-2}$ s, $t_4 = 1.043 \cdot 10^{-1}$ s, $t_5 = 1.077 \cdot 10^{-1}$ s, $t_6 = 1.144 \cdot 10^{-1}$ s)

Vertical displacement of the middle point is shown as a function of time in Figure 6. Response according to both approaches is the same until the disappearance of the element attached to this node.

5.2. Case 2: a clamped plate

Analysis similar to that of the hinged plate has been performed for a clamped plate (see Figures 8 and 9). In this case, the evolution of inelastic strains begins at

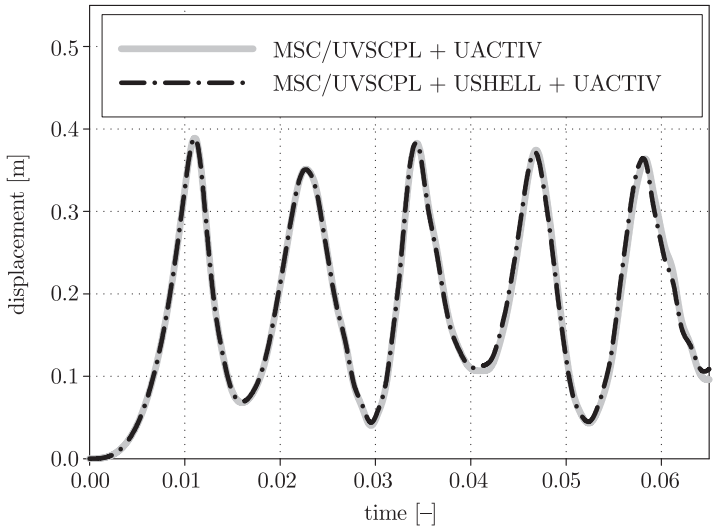

Figure 6. Time functions of the middle point vertical vibrations for the hinged plate

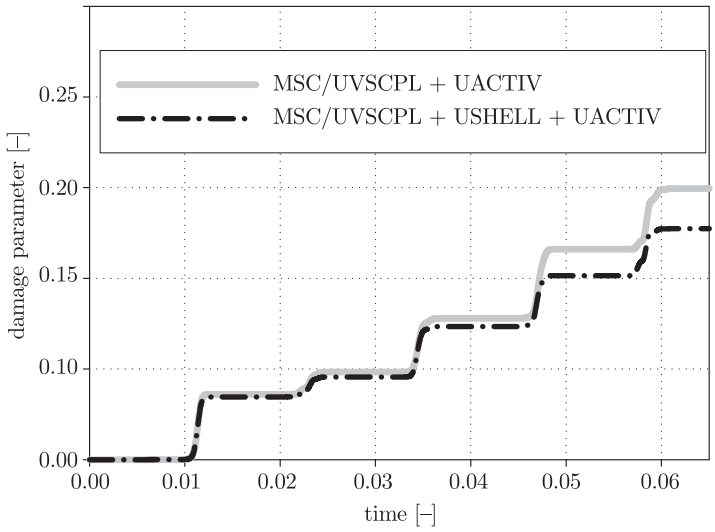

Figure 7. Time functions of the middle point damage evolution for the hinged plate

the plate's edges; therefore, the edge finite elements are re-meshed first, following which, the middle part of the plate's quarter is re-meshed. Additionally, elimination of damaged elements begins close to the clamped edges. In the classical approach, elements in the middle of the edge are eliminated first, wherefrom elimination progresses towards the plate's corners, so that finally almost the entire plate is separated (Figure 8, $t_5 = 2.907 \cdot 10^{-2}$s). However, in the change of thickness approach, elements close to plate's corners are deactivated first, and damage progresses along the edge to its centre. The ultimately separated part is very similar to the other approach. The time-displacement functions for the plate's middle point are also insensitive to the approach (Figure 10).

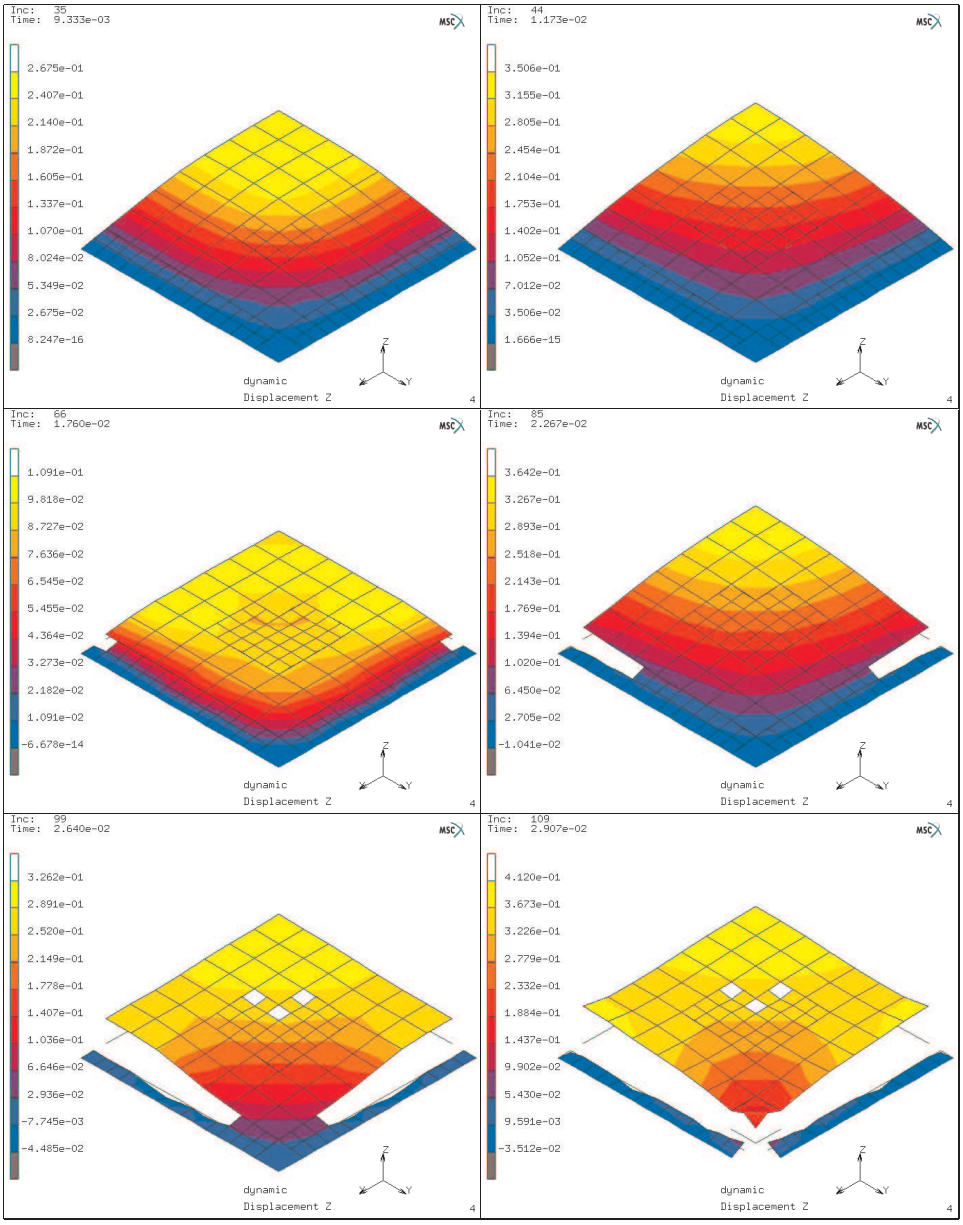

Figure 8. Clamped plate: damage analysis with subroutines UVSCPL + UACTIV ($t_1 = 9.333 \cdot 10^{-3}$ s, $t_2 = 1.173 \cdot 10^{-2}$ s, $t_3 = 1.76 \cdot 10^{-2}$ s, $t_4 = 2.267 \cdot 10^{-2}$ s, $t_5 = 2.64 \cdot 10^{-2}$ s, $t_6 = 2.907 \cdot 10^{-2}$ s)

6. Conclusions

Numerical examples have been presented in the framework of the first-order shear deformation and geometrically non-linear shell theory, under the small-strain assumption. The obtained results encourage the authors to continue the research on the basis of extended experimental data. The present work is the first step of a comprehensive investigation of damage evolution.

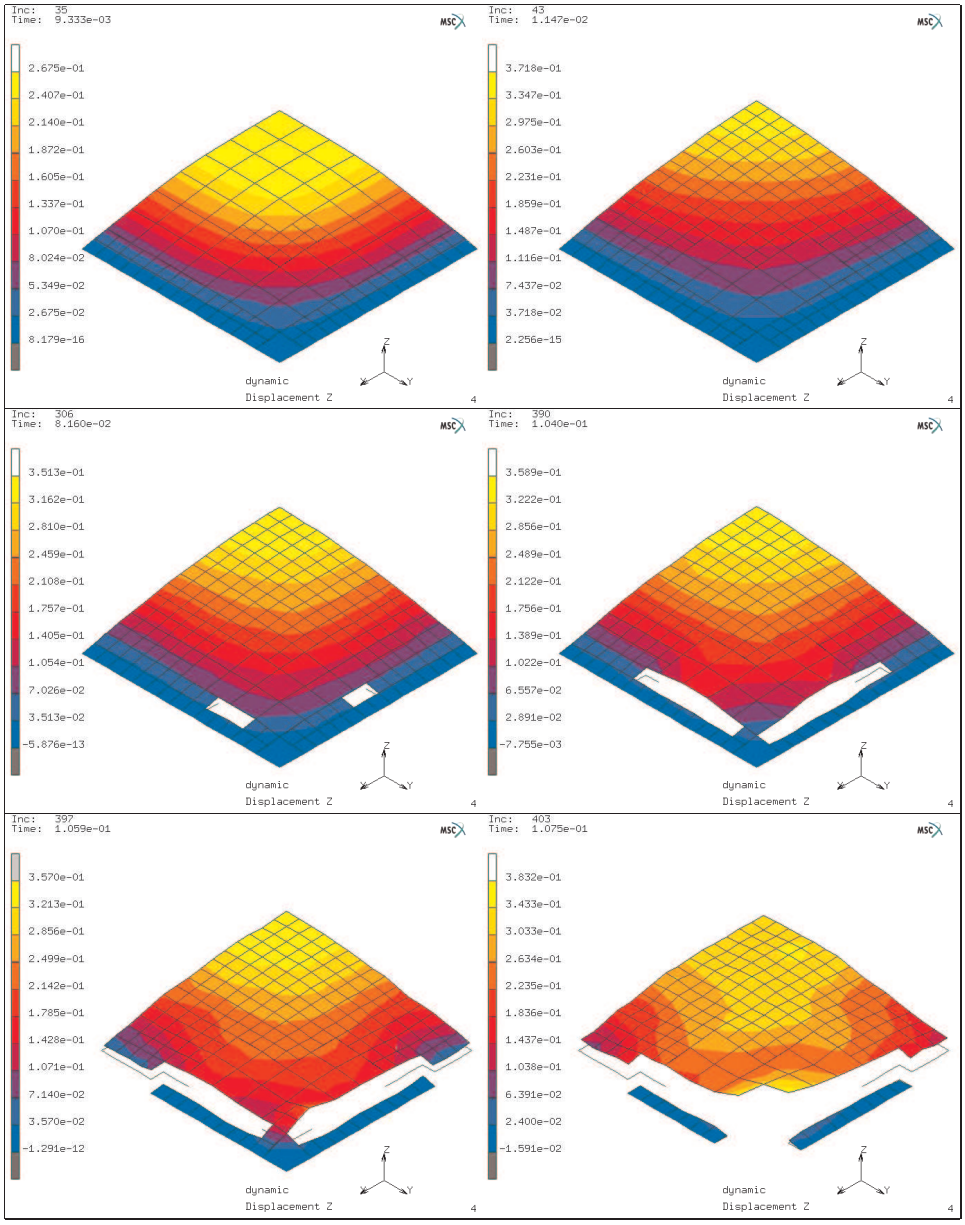

Figure 9. Clamped plate: damage analysis with subroutines UVSCPL + USHELL + UACTIV ($t_1 = 9.333 \cdot 10^{-3}$ s, $t_2 = 1.147 \cdot 10^{-2}$ s, $t_3 = 8.16 \cdot 10^{-2}$ s, $t_4 = 1.04 \cdot 10^{-1}$ s, $t_5 = 1.059 \cdot 10^{-1}$ s, $t_6 = 1.075 \cdot 10^{-1}$ s)

The applied numerical improvements have extended the range of performed analysis in comparison with the approach where calculations collapse when damage function D has a value close to 1 at a single integration point. Both approaches have generally produced similar answers, in spite of the different physical meaning of the two types of calculations. Re-meshing of the original finite element mesh due to dependency of new nodes can also increase the calculations' range. In dynamic

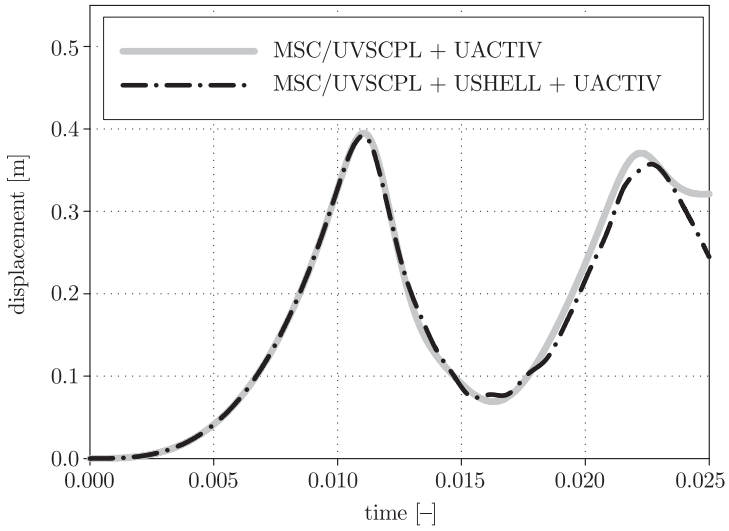

Figure 10. Time functions of the middle point vertical vibrations for the clamped plate

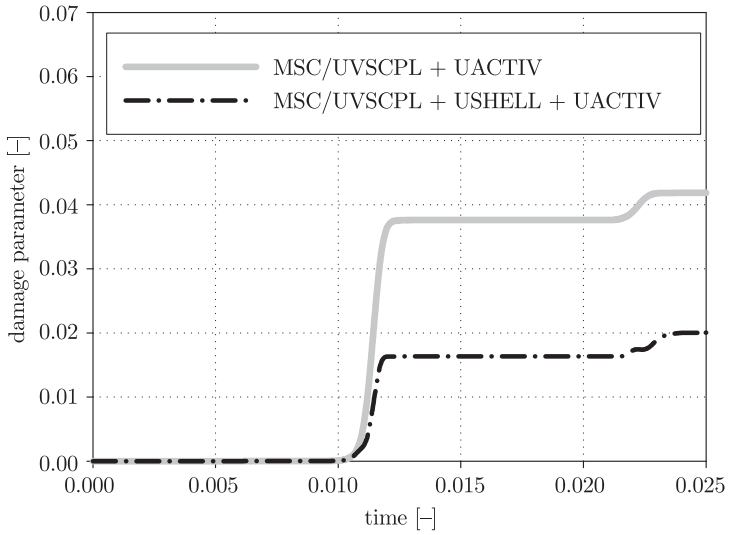

Figure 11. Time functions of the middle point damage evolution for the clamped plate

calculations, separated elements of the structure are capable of rigid movements, which can be traced by non-linear dynamic algorithms.

Acknowledgements

Calculations presented in the paper were performed at the Academic Computer Centre in Gdansk (TASK) and the RWTH Aachen Centre.

The research was a part of the DAAD 2004/2005 Polish-German cooperation programme (KBN/DAAD 2004/2005 no. 09).

References

[1] Perzyna P 1963 *Quart. of Appl. Mech.* **20** 321

[2] Chaboche J-L 1989 *Int. J. of Plasticity* **5** 247
[3] Woznica K and Kłosowski P 2000 *Arch. of Appl. Mech.* **70** 561
[4] Ambroziak A and Kłosowski P 2006 *Task Quart.* **10** (1) 49
[5] Lemaitre J 1985 *J. of Engin. Materials and Technology* **107** 83
[6] Bonora N 1997 *Engin. Fracture Mech.* **58** 11
[7] Chandrakanth S and Pandey P C 1995 *Int. J. of Fracture* **72** 293
[8] Chandrakanth S and Pandey P C 1995 *Engin. Fracture Mech.* **50** 457
[9] Dhar S Sethuraman R and Dixit P M 1996 *Engin. Fracture Mech.* **53** 917
[10] Tai W H and Yang B X 1986 *Engin. Fracture Mech.* **25** 377
[11] Wang T-J 1995 *Engin. Fracture Mech.* **51** 275
[12] Xiao Y C, Li S and Gao Z 1998 *Int. J. of Fatigue* **20** 503
[13] Lemaitre J and Chaboche J L 1990 *Mechanics of Solid Materials*, Cambridge University Press, Cambridge
[14] Ammar G and Dufailly J 1993 *European J. of Mech., A/Solids* **12** 197
[15] Users handbook: MSC.MARC Volume D: User Subroutines and Special Routines, Version 2005. MSC.Software Corporation 2005
[16] Ambroziak A 2005 *Task Quart.* **9** 157
[17] Users handbook: MSC.MARC Volume B: Element Library, Version 2005. MSC.Software Corporation 2005
[18] Newmark N M 1959 *J. of the Engin. Mech. Division* **85** 67